AD-A116 937 WISCONSIN UNIV-MADISON DEPT OF PHYSICS F/G 20/6
PULSED EXCITATION AND COLLISIONAL PROCESSES.(U)
APR 82 L W ANDERSON, C C LIN F19628-78-C-0042
UNCLASSIFIED AFGL-TR-82-0139 NL

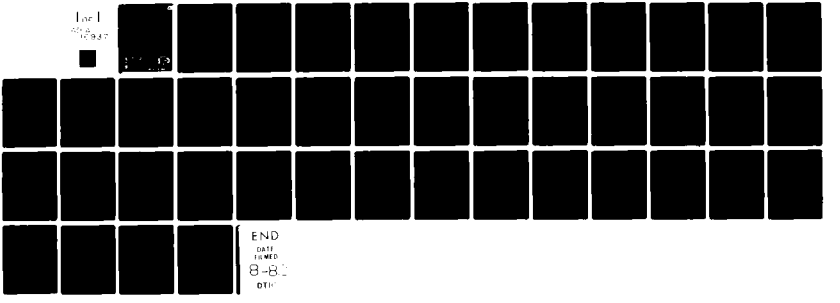

END
DATE FILMED
8-82
DTIC

AD A116937

[redacted]

[redacted]

L. E. Holzworth
C. C. Lin

Department of Physics
University of Wisconsin-Madison
Madison, Wisconsin 53706

Final Report
1 January 1978 - 31 March 1982

29 April 1982

Approved for public release; distribution unlimited

[redacted]

DTIC
S ELECTE

Unclassified

SECURITY CLASSIFICATION OF THIS PAGE (When Data Entered)

REPORT DOCUMENTATION PAGE		READ INSTRUCTIONS BEFORE COMPLETING FORM
1. REPORT NUMBER AFGL-TR-82-0139	2. GOVT ACCESSION NO. AD-A116 937	3. RECIPIENT'S CATALOG NUMBER
4. TITLE (and Subtitle) Pulsed Excitation and Collisional Processes		5. TYPE OF REPORT & PERIOD COVERED Final 1 January 1978 - 31 March 1982 6. PERFORMING ORG. REPORT NUMBER
7. AUTHOR(s) L. W. Anderson C. C. Lin		8. CONTRACT OR GRANT NUMBER(s) F19628-78-C-0042
9. PERFORMING ORGANIZATION NAME AND ADDRESS Department of Physics University of Wisconsin-Madison Madison, Wisconsin 53706		10. PROGRAM ELEMENT, PROJECT, TASK AREA & WORK UNIT NUMBERS 61102F 2310G4AH
11. CONTROLLING OFFICE NAME AND ADDRESS Air Force Geophysics Laboratory Hanscom AFB, Massachusetts 01731 Monitor/Edward T. P. Lee/OPR		12. REPORT DATE 29 April 1982 13. NUMBER OF PAGES 44
14. MONITORING AGENCY NAME & ADDRESS(if different from Controlling Office)		15. SECURITY CLASS. (of this report) Unclassified 15a. DECLASSIFICATION/DOWNGRADING SCHEDULE

16. DISTRIBUTION STATEMENT (of this Report)

Approved for public release; distribution unlimited

17. DISTRIBUTION STATEMENT (of the abstract entered in Block 20, if different from Report)

18. SUPPLEMENTARY NOTES

19. KEY WORDS (Continue on reverse side if necessary and identify by block number)

collisional quenching, laser-induced fluorescence, the $a^3\Sigma_u^+$ and $d^3\Sigma_u^+$ levels of the He_2 molecule, the $a^3\Sigma_u^+$ level of the N_2 molecule.

20. ABSTRACT (Continue on reverse side if necessary and identify by block number)

The method of pulsed excitation is used to study the rates of population and de-population of energy levels of molecules. Optical measurements are made with the aid of laser-spectroscopic techniques. Application to a helium discharge yields collisional quenching rates. Preliminary studies on nitrogen molecules are reported.

DD FORM 1 JAN 73 1473 EDITION OF 1 NOV 65 IS OBSOLETE

Unclassified

SECURITY CLASSIFICATION OF THIS PAGE (When Data Entered)

Chapter I.

Introduction

In this project we utilize the method of pulse excitation to study atomic and molecular processes. The primary excitation is produced by a pulsed gas discharge. After the cessation of the pulse, the populations of the various excited levels are monitored. From the time-dependence of these populations, it is possible to determine rate constants for production and decay of different excited species through collisional transfer. The pulse method has an advantage over measurements in the steady state in that we can study transfer processes without the influence of the primary excitation. For probing the populations of the excited levels we use the technique of laser spectroscopy to isolate the individual levels.

To develop and perfect the necessary techniques for experimental measurement and data analysis appropriate to the conditions or our work, we perform the pulse excitation experiment for a helium discharge. Since a great deal is known about the transfer processes in a helium discharge, we can compare our results with those of other researchers. In Chapters II and III we describe our study on helium discharge. Where our results overlap with those of earlier works, we generally find good agreement. However, our experiments also provide rate constants that have not been measured previously. Furthermore our work on helium shows that the use of pulse excitation along with laser spectroscopy is an effective way to study excitation transfer processes. In Chapter IV we report our efforts to adopt this scheme to study excitation processes for nitrogen molecules.

Chapter II.

$He_2(d^3\Sigma_u^+)$ decay rate in a high-pressure helium afterglow

The development of atmospheric pressure lasers has illuminated the continuing need for the study of collisional processes in high pressure afterglows. In this paper we report the first measurement of the pressure dependent $He_2(d^3\Sigma_u^+)$ decay in the afterglow of a helium discharge at pressures from 50 to 700 Torr. The measured total collisional quenching rate for the (v = 0) $He_2(d^3\Sigma_u^+)$ molecule by $He(1^1S)$ is $(2.5 \pm 0.2) \times 10^{-12}$ cm^3 sec^{-1} at 293°K. This corresponds to a thermally averaged cross section of 0.16×10^{-16} cm^2. This work complements an earlier paper[1] which reported a total collisional quenching rate for $He(3^3S)$ level atoms by ground state He atoms of $(6.4 \pm 0.3) \times 10^{-12}$ cm^3 sec^{-1} at 292°K.

The experimental technique is based upon dye-laser induced fluorescence. Metastable $He_2(a^3\Sigma_u^+)$ molecules created in the afterglow of the discharge are excited to the $e^3\Pi_g$ level by a dye-laser pulse. Collisions rapidly transfer some of the $e^3\Pi_g$ molecules to the $d^3\Sigma_u^+$ level. The temporal dependence of the resulting $d^3\Sigma_u^+ \rightarrow b^3\Pi_g$ fluorescence is then measured. A schematic drawing of the apparatus is shown in Fig. 1. A Tektronics 115 pulse generator supplies a pair of timing pulses. The first pulse triggers the thyratron-switched He discharge; the second pulse, after a variable delay of 50 to 100 μsec, triggers a thyratron-switched nitrogen laser that pumps a dye laser. The 0.05 nm bandwidth, 3 nsec duration dye laser pulse[2] is tuned to the Q5 line of the (0-0) band of the He_2 $e^3\Pi_g \leftarrow a^3\Sigma_u^+$ transition at 465.2 nm. After collimation to a beam diameter of 3.5 mm, the 5 μJ dye laser pulse is passed twice through the afterglow. The laser induced fluorescence from the (0-0) band of the $d^3\Sigma_u^+ \rightarrow b^3\Pi_g$ transition at 640 nm is imaged with 1:1 magnification using an f/4 lens onto an EMI 9785B photomultiplier. The photomultiplier signal is large enough to be clearly displayed on a Tektronics 475 oscilloscope. Individual

oscilloscope traces are photographed, digitized, and analyzed to determine the temporal characteristic of the fluorescence.

At each pressure the time delay between the He discharge pulse and the dye laser excitation pulse is increased until the observed $d^3\Sigma_u^+$ decay rate is independent of the delay time. This ensures that remenant plasma ionization and recombination does not effect the measured decay rate. Further increases in the delay time resulting in decreases of the $He_2(a^3\Sigma_u^+)$ and $He(2^3S)$ level populations by factors of up to 20 produce no change in the observed decay rate. This indicates metastable He atoms and molecules do not effect the measurement. Typical $He_2(a^3\Sigma_u^+)$ densities for a time delay of 100 μsec are 10^{10} to 10^{11} cm^{-3}. At the pressures used in this experiment, the population of the $He_2(e^3\Pi_g)$ level produced by the dye laser pulse is collisionally quenched in a time comparable to or shorter than the duration of the dye laser pulse.[3] The observed rise time of the 640 nm fluorescence is essentially the same as the convolted rise times of the photomultiplier and the dye laser pulse. The transfer rate of $d^3\Sigma_u^+$ level molecules back to the $e^3\Pi_g$ level is negligible at thermal energies because the $d^3\Sigma_u^+$ level lies 0.15 eV below the $^3\Pi_g$ level. We have measured the rotational temperature of the $He_2(a^3\Sigma_u^+)$ molecules as a function of the time. These molecules are created rotationally hot, but they cool to near room temperature within 100 to 150 μsec. For this reason we take the neutral gas temperature to be room temperature.

The possible influence of impurities upon the measured pressure dependent decay rate must be considered. This is hampered by the lack of theoretical or experimental knowledge of the reaction kinetics of nonmetastable He_2 molecules. The strong Rydberg nature of He_2 molecules[4,5] results in similar reaction rates, normally within a factor of 3, for the quenching of $He_2(a^3\Sigma_u^+)$

and of $He(2^3S)$ by impurities.[6-8] Present rate data indicate the 3^3S atoms are only a few times more reactive than the 2^3S metastable atoms when chemionization is an open reaction channel.[9,10] By analogy we expect the $d^3\Sigma_u^+$ reaction rates with impurities to be only slightly larger than the $a^3\Sigma_u^+$ reaction rates. The $a^3\Sigma_u^+$ decay rate measured in our system is always at least a factor of 400 slower than the measured $d^3\Sigma_u^+$ decay rate. For this reason we feel the impurities do not make a significant contribution to the observed $d^3\Sigma_u^+$ quenching rates.

The $He_2(d^3\Sigma_u^+)$ decay rate as a function of the pressure is shown in Fig. 2. Each datum point for the $He_2(d^3\Sigma_u^+)$ decay curve is obtained by averaging the decay rates obtained from seven to 15 oscilloscope trace photographs of the 640 nm fluorescence signal. The error bars represent one standard deviation in the data. Using a least-squares fit to the expression $R = a + bP$, we obtain $a = (1.98 \pm 0.14) \times 10^7$ sec^{-1} and $b = (8.2 \pm 0.6) \times 10^4$ Torr^{-1} sec^{-1}. The slope represents a total collisional quenching rate for the $d^3\Sigma_u^+$ molecule of $(2.5 \pm 0.2) \times 10^{-12}$ cm^3 sec^{-1} at 293°K and the intercept gives the radiative decay rate of the $d^3\Sigma_u^+$ level. There is no previous measurement of the $d^3\Sigma_u^+$ collisional quenching rate. The measurements of Delpech, Gauthier, and Devos taken between 8 and 34 Torr indicated a pressure independent decay rate of $(2.15 \pm 0.15) \times 10^{-7}$ sec^{-1} for the isotopically rare $^3He_2(d^3\Sigma_u^+)$ electronic state.[11] The radiative decay rate of an electronic level should be the same for $^3He_2$ and $^4He_2$ and collisional quenching rates of the $d^3\Sigma_u^+$ level molecules of $^3He_2$ and $^4He_2$ by ground state He atoms should be similar. Within the uncertainty of their experiment, decay rates predicted by our experiments and analysis agree with the results of Delpech et al. when our experiments are extrapolated to the pressures used by Delpech et al.

The lack of three body potential surfaces for He_3 prevents a definite theoretical prediction of the reaction pathways in the collisional quenching of $He_2(d^3\Sigma_u^+)$ molecules by thermal $He(1^1S)$ atoms. The probable reaction products may be conjectured by using as guidelines conservation of spin, access to only energetically allowed levels, and magnitude of energy defect between initial and final states. Possible products would then be two $He(1^1S)$ atoms plus a $He(2^3S)$ atom or one $He(1^1S)$ atom plus either a He_2 $a^3\Sigma_u^+$, $b^3\Pi_g$, or $c^3\Sigma_g^+$ molecule. The energy defect between the (v = 0) $d^3\Sigma_u^+$ level and the highest vibrational level of the $c^3\Sigma_g^+$ molecule is more than 0.5 eV. The $2^3S + 1^1S$ dissociation limit of the $a^3\Sigma_u^+$ level molecule is about 0.8 eV below the (v = 0) $d^3\Sigma_u^+$ level. For these channels kinetic energy of the products must take up rather large amounts of energy. However, the (v = 0) $d^3\Sigma_u^+$ level, which lies about 0.25 eV below the $2^3P + 1^1S$ dissociation limit of the $b^3\Pi_g$ molecule, is nested among the high lying $b^3\Pi_g$ vibrational levels. Atom exchange collisions between $He(1^1S)$ atoms and $He_2(d^3\Sigma_u^+)$ molecules could be effective in producing these vibrationally excited $b^3\Pi_g$ molecules. Of course, it may be possible to produce He_2 in the $c^3\Sigma_g^+$ state or in the low vibrational levels of the $b^3\Pi_g$ state via crossings of the appropriate potential surfaces of the He_3 system. In the absence of any detailed information on such potential surfaces, we are not able to comment on the likelihood of these mechanisms. Nevertheless, it is interesting to note that the valence electron of $He_2(d^3\Sigma_u^+)$ is largely 3s-like and that the quenching rate for the $He(3^3S)$ atom (6.4×10^{12} cm^3sec^{-1})[1] is indeed rather close to that of the $He_2(d^3\Sigma_u^+)$ molecule. Based on theoretical calculations it is believed that a major quenching mechanism for the $He(3^3S)$ atom is the nonresonant $3^3S - 2^3P$ excitation transfer due to the

curve crossing of the $f^3\Sigma_u^+$ and $d^3\Sigma_u^+$ potentials.[4] Thus, one may speculate analogous kinds of potential surface crossings for the He_3 system which may result in nonresonant $d^3\Sigma_u^+ - c^3\Sigma_g^+$ and $d^3\Sigma_u^+ - b^3\Pi_g$ collisional transfer.

References

1. J. E. Lawler, J. W. Parker, L. W. Anderson, and W. A. Fitzsimmons, Phys. Rev. A 19, 156 (1979).
2. J. E. Lawler, W. A. Fitzsimmons, and L. W. Anderson, Appl. Opt. 15, 1083 (1976).
3. J.-C. Gauthier, J.-P. Geindre, J.-P. Moy, and J.-F. Delpech, Phys. Rev. A 13, 1781 (1976).
4. W. S. Steets and N. F. Lane, Phys. Rev. A 11, 1994 (1975).
5. J. S. Cohen, Phys. Rev. A 13, 86 (1976).
6. F. W. Lee and C. B. Collins, J. Chem. Phys. 65, 5189 (1976).
7. F. W. Lee and C. B. Collins, J. Chem. Phys. 67, 2798 (1977).
8. F. W. Lee, C. B. Collins, L. C. Pitchford, and R. Deloch, J. Chem. Phys. 68, 3025 (1978).
9. S. Kubota, C. Davies, and T. A. King, J. Phys. B 8, 1220 (1975).
10. A. L. Schmeltekopf and F. C. Fehsenfeld, J. Chem. Phys. 53, 3173 (1970).
11. J.-F. Delpech, J.-C. Gauthier, and F. Devos, J. Chem. Phys. 67, 5934 (1977).

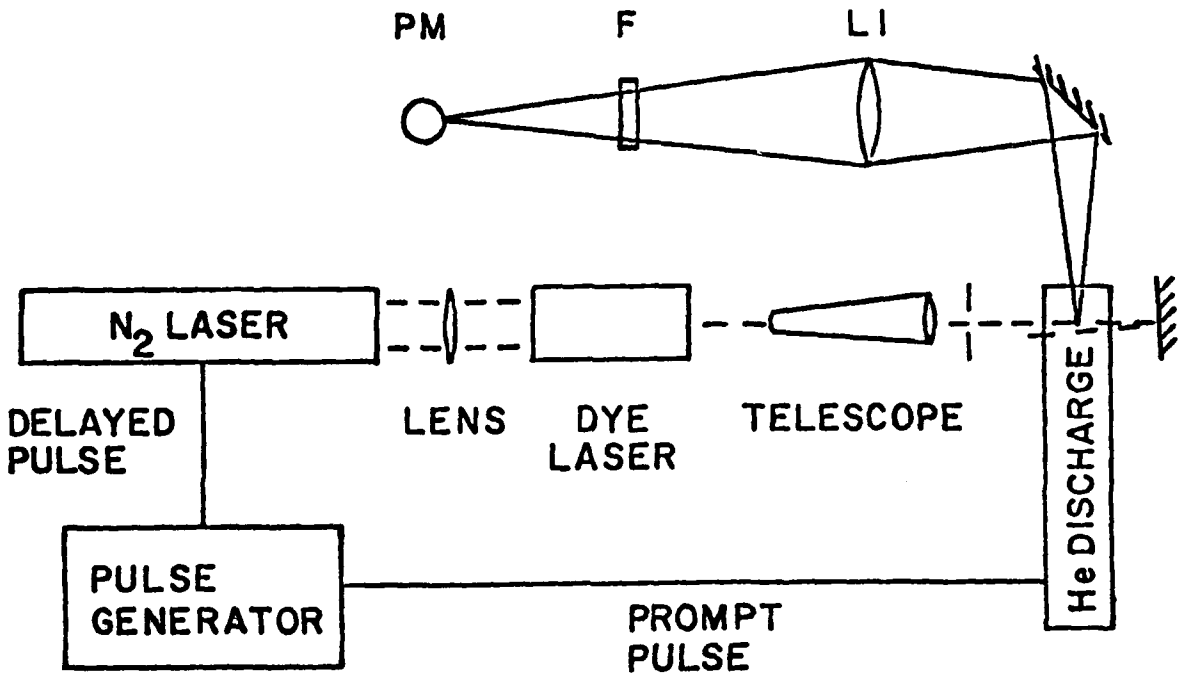

FIG. 1. Schematic diagram of the experimental apparatus. A N_2 laser pumps a dye laser. The dye-laser radiation is collimated by a telescope and then passed through the He discharge. Dye-laser induced fluorescence is imaged onto the cathode of a photomultiplier tube PM by lens L1.

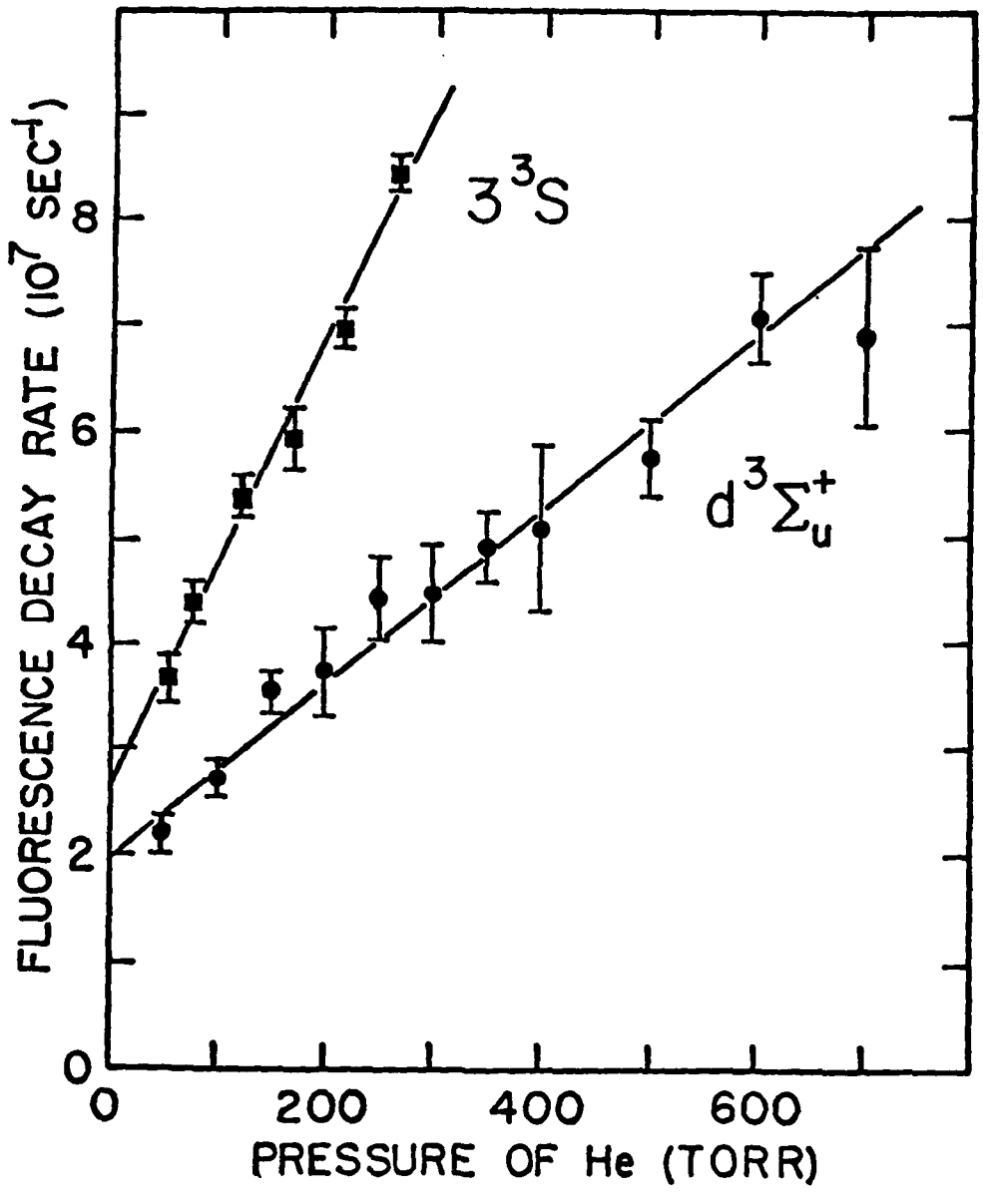

FIG. 2. Decay rates of the $He_2(d^3\Sigma_u^+)$ level as a function of discharge cell pressure. A least-squares fit of the $He_2(d^3\Sigma_u^+)$ decay rate to the equation a + bP gives a=(1.98±0.14) x 10^7 sec^{-1} and b=(8.20±0.55)x10^4Torr^{-1} sec^{-1} at 293°K. Also shown are the decay rates of the He(3^3S) level from Ref. 1. A fit to the He(3^3S) decay rate gives a=(2.63±0.20)x10^7 sec^{-1} and b=(2.12±0.11) x 10^5 Torr^{-1}sec^{-1}. The error bars represent one standard deviation in the data.

Chapter III.

Collisional quenching of He_2 molecules in the $a^3\Sigma_u^+$ level by impurity gases

I. Introduction

This chapter reports measurements of the rate constants (at room temperature) for the collisional quenching of He_2 molecules in the $a^3\Sigma_u^+$ level by Ar, N_2, O_2, H_2, and CO_2. The diatomic He_2 molecule has a strong Rydberg character,[1,2] and there is a close correspondence between the $a^3\Sigma_u^+$ level of the He_2 molecule and the 2^3S level of the He atom. Hence, the measurements reported in this paper parallel the measurements of the rate constants for the collisional quenching of the $He(2^3S)$ level by various atoms and molecules.[3,4,5,6]

Our measurements are performed in the afterglow of a pulsed He discharge at pressures of 200 and 300 Torr. Metastable $He_2(a^3\Sigma_u^+)$ molecules are created in the afterglow of the pulsed discharge predominantly through the recombination of molecular He_2^+ ions and through the conversion of metastable $He(2^3S)$ atoms into $He(a^3\Sigma_u^+)$ molecules by the reaction $He(2^3S) + 2He \rightarrow He(a^3\Sigma_u^+) + He$.

Some of the $He_2(a^3\Sigma_u^+)$ molecules are excited to the $e^3\pi_g$ level by a pulse of light from a N_2 laser-pumped dye laser tuned to 465 nm, the wavelength of the Q5 line of the (0-0) band of the $e^3\pi_g \leftarrow a^3\Sigma_u^+$ transition. Collisions with ground state He atoms rapidly transfer some of the $e^3\pi_g$ molecules to the $d^3\Sigma_u^+$ level. The resulting fast fluorescence on the $d^3\Sigma_u^+ \rightarrow b^3\pi_g$ transition at 640 nm is monitored. The optical absorption, collisional transfer, and optical emission are shown in Fig. 1. The change in the fluorescence yield as the delay between pulsing the He discharge and pulsing the N_2 pumped dye laser increases is used to monitor the change of the population of the $a^3\Sigma_u^+$ molecules. The collisional quenching rate of the $He_2(a^3\Sigma_u^+)$ molecules is measured at different concentrations of foreign gas yielding Stern-Volmer plots[7] of the $a^3\Sigma_u^+$ quenching rate as a function of the foreign gas concentration.

There are two previous measurements of the collisional quenching rate of the $He_2(a^3\Sigma_u^+)$ level by a foreign gas. Lee and Collins[8] have measured the rate constants for the quenching of $He_2(a^3\Sigma_u^+)$ molecules by Ne, Ar, N_2, CO, CO_2, and CH_4 in the afterglow of an electron-beam generated discharge at He pressures from 1,500 to 2,500 Torr. They present their measurements as effective rate constants since at the high pressures of their experiment three body collisions among $He_2(a^3\Sigma_u^+)$ molecules, foreign gas molecules, and $He(1^1S)$ atoms account for 30 to 50% of the quenching collisions. Pitchford and Deloche[9] have measured the rate constant for quenching of $He_2(a^3\Sigma_u^+)$ molecules by Ar at He pressures below 60 Torr.

In the present work, we combine our data for Ar, N_2, and CO_2 taken in the afterglow of a He discharge at pressures of 200 and 300 Torr with the data of Lee and Collins to extract both bimolecular and termolecular rate constants. A similar analysis has been used by Lee, Collins, Pitchford, and Deloche[10] to obtain bimolecular and termolecular rate constants for the quenching of $He_2(a^3\Sigma_u^+)$ molecules by Ar.

II. Experimental Apparatus and Method

A schematic drawing of our experimental apparatus is shown in Fig. 2. The Tektronic 115 pulse generator supplies a pair of +2V, 10 nsec duration, timing pulses at a 10 Hz repetition rate. The first pulse triggers the thyratron-switched He discharge; the second pulse triggers the thyratron-switched N_2 laser that pumps the dye laser. The 0.05 nm bandwidth, 3 nsec pulse duration dye laser is tuned to the 465.2nm Q5 line of the (0-0) band of the He_2 $e^3\pi_g \leftarrow a^3\Sigma_u^+$ transition. After collimation to a beam diameter of 3.5 mm, the 5 μJ dye laser pulse passes through the center of the discharge region and then reflects off a mirror back through the discharge at a small angle to its

original path. A lens stopped to f/4 images the laser-induced fluorescence of the (0-0) band of the $d^3\Sigma_u^+ \rightarrow b^3\pi_g$ transition at 640 nm onto an EMI 9684B photomultiplier with 1:1 magnification. The dye laser pulse strongly saturates the $e^3\pi_g \leftarrow a^3\Sigma_u^+$ transition. The amount of laser induced fluorescence is proportional to the concentration of $a^3\Sigma_u^+$ (v=0, J=5) molecules. The fluorescence signal is displayed on a Tektronix 475 oscilloscope.

The $a^3\Sigma_u^+$ decay rate is measured as follows: A neutral density filter of 5 or 10% transmission is located between the discharge and photomultiplier. The delay between the He discharge and the N_2 laser discharge is adjusted so that the fluorescence signal is near the upper end of the photomultiplier's linear region. As the delay increases, neutral density filters of higher transmission are substituted so that the peak signal currents remain between 0.15 and 0.4 mA. The scan ends when the delay becomes so long that the peak current drops below 0.15 mA with no neutral density filter present. The increment in delay is chosen so that the fluorescence signal is measured 8 to 12 times during a scan. The delay is measured with an accuracy of ±0.5%.

The time dependence of the fluorescence signal is exponential and the time constant does not change as the delay increases. The amount of laser-induced fluorescence is proportional to the peak height of the photomultiplier signal observed on the Tektronic 475 oscilloscope. At each delay the peak heights, which vary by 10 - 15% from pulse to pulse, are averaged by eye. The peak heights are normalized by dividing the measured peak height by the transmission of the neutral density filter at 640 nm. The normalized data are then graphed on semi-log paper resulting in a plot like that shown in Fig. 3. For each scan a least-squares fit of the normalized data to an expression of the form $ae^{xp}(-bt)$ is performed where t is the time in seconds.

For each foreign gas, four samples of foreign gas-He mixture of varying concentration are prepared. The preparation of the gas mixture is done over a six day period. We start with a full size 1A cylinder of 99.995% purity He gas (43.8 liter internal volume pressurized to about 2,400 psi). On the first day, the decay rates of the $a^3\Sigma_u^+$ level in a 200 and in a 300 Torr He discharge are measured for the source cylinder. Each of the four succeeding days a sample is prepared by filling a cylinder evacuated to a pressure of a few m Torr to a pressure of several Torr of the foreign gas and then to a total pressure of 316 psi with He from the source tank. The foreign gas pressure in the second, third, and fourth mix cylinders are nominally 2, 3, and 4 times that of the first. On the sixth day, the $a^3\Sigma_u^+$ decay rates in a 200 and in a 300 Torr He discharge are again measured for the source cylinder. The source cylinder decay rate increases from values of $0.5\text{-}1.0 \times 10^5$ sec^{-1} initially on day 1 to $1.0\text{-}2.0 \times 10^5$ sec^{-1} on day 6 after the filling of the 4 mix cylinders. We do not know why the background decay rate increases with time, but we speculate that the He tank may have a contaminent with a constant vapor pressure so that the contaminant fraction increases as He is withdrawn from the tank. We assume in the data analysis that the background rate of the source tank increases linearly with time as the tanks are filled. We estimate that this assumption contributes only about a 5% uncertainty to the rate constants measured.

III. Rate Constants for Collisional Quenching of $He_2(a^3\Sigma_u^+, v = 0)$ Molecules by Ar, N_2, O_2, H_2, and CO_2

The rate equation describing the evolution of the $a^3\Sigma_u^+$ population during the afterglow is given by:

$$\frac{-1}{[M]}\frac{d[M]}{dt} = \nu + K_2[X] + K_3[X]\ [He], \tag{1}$$

or

$$\frac{-1}{[M]}\frac{d[M]}{dt} = \nu + K[X] \tag{2}$$

where [M], [X], and [He] are, respectively, the concentrations of $He_2(a^3\Sigma_u^+, v = 0)$ molecules, the added foreign gas, and the He (1^1S) atoms, K_2 is the bimolecular rate constant, K_3 is the termolecular rate constant for the destruction of $a^3\Sigma_u^+$ molecules by foreign gas X, and $K = K_2 + K_3[He]$ is the effective rate constant. The rate ν represents loss and source terms due to other processes that affect the $a^3\Sigma_u^+$ population. Loss terms include diffusion of $a^3\Sigma_u^+$ molecules out of the discharge region and collisions between the $a^3\Sigma_u^+$ molecules and impurities in the helium, other $a^3\Sigma_u^+$ molecules, $He(2^3S)$ metastable atoms, and electrons. Source terms include recombination of He_2^+ ions and collisions of $He(2^3S)$ atoms with two $He(1^1S)$ atoms. The data analysis assumes that the rates encompassed under ν are either constant during the afterglow or of such small size compared to the total $a^3\Sigma_u^+$ decay rate that they are negligible. This assumption is justified in Ref. 11.

The fractions of $a^3\Sigma_u^+$ molecules in the lower J levels at various delay times are measured by pumping the Q1, Q3, Q5, and Q7 lines of the e ← a transition with the dye laser. An approximate rotational temperature is calculated from the measured fluorescence signals for the various rotational levels. At all times the rotational populations are nearly represented by a Boltzmann distribution. The $a^3\Sigma_u^+$ molecules are created rotationally hot with a rotational temperature of about 400°K at the shorter delays and cool to near room temperature within 100 to 150 μsec in agreement with observations by Callear and Hedges.[12] The population of the J = 5 level is nearly independent of the temperature for a Boltzmann distribution; for example the fraction of the $a^3\Sigma_u^+$ population in the J = 5 level is 0.262 at 400°K and is 0.266 at 290°K for a Boltzmann distribution. The measured ratios of the fluorescence signals show that the fraction of the $a^3\Sigma_u^+$ population in the J = 5 level is nearly independent of the delay decreasing slightly from 0.30 ± 0.01 at a delay of about 20 μsec to 0.28 ± 0.01 at 90 μsec. Thus the measured populations for the J = 5 level are in reasonable agreement with the populations calculated using a Boltzmann distribution and our measured temperature as a function time. Since the rotational temperature cools to room temperature, we take the neutral gas kinetic temperature to be room temperature 295 ± 7°K.

In our analysis we neglect several effects that can cause systematic errors. The systematic errors in this experiment are estimated to be about 10% for electron+He_2^+ recombination producing $a^3\Sigma_u^+$ (v = 0) molecules, 6% for the change in the ratio of the concentration of $a^3\Sigma_u^+$ (v = 0, J = 5) molecules to the total $a^3\Sigma_u^+$ (v = 0) concentration, 5% for the conversion of

$He(2^3S)$ metastable atoms directly producing $a^3\Sigma_u^+$ (v = 0) molecules, 2% for electron-He_2 ($a^3\Sigma_u^+$) collisions that depopulate the $a^3\Sigma_u^+$ (v = 0) level, and 1% for $He(2^3S)$-$He_2(a^3\Sigma_u^+)$ collisions that depopulate the $a^3\Sigma_u^+$ (v = 0) level. Thus there is a 20% uncertainty in our measurement due to systematic errors. Although there is no direct measurement of the vibrational distribution of $a^3\Sigma_u^+$ molecules produced by the reaction

$$He(2^3S) + 2He(1^1S) \rightarrow He_2(a^3\Sigma_u^+) + He(1^1S) \qquad (3)$$

it is expected that the $He_2(a^3\Sigma_u^+)$ molecules will be created mostly in high vibrational levels. If the fraction of $a^3\Sigma_u^+$ molecules produced in the v = 0 vibrational level is non-negligible, the conversion of $He(2^3S)$ atoms to $He_2(a^3\Sigma_u^+)$ molecules will represent a long-lived source of $a^3\Sigma_u^+$ molecules in the afterglow that will affect the measured $a^3\Sigma_u^+$ decay rate.

A Stern-Volmer[7] plot of H_2 partial pressure against $He_2(a^3\Sigma_u^+, v = 0)$ decay rate is shown in Fig. 4. For this figure, each datum point in the upper plot is the average value of the decay rates measured in 4 to 6 data scans. The error bar for each point is determined by adding in quadrature the standard deviation of the average decay rate and the average uncertainty in the fitted decay rate of each scan. The data points at zero partial pressure are background decay rates for the helium from the source tank before and after the mix tanks are filled. After the background rate is subtracted from the average rate, the reduced data, shown in the lower plot, at 200 and 300 Torr are separately fitted to the expression $R = a + bP$ where R is the decay rate and P is the foreign gas partial pressure. The least-squares fit generates the dashed and solid lines shown in the figures. The slope of each line gives the rate constant for quenching of $He_2(a^3\Sigma_u^+, v = 0)$ molecules by

collisions with the foreign gas. The effective rate constant K, listed in Table 1 for each foreign gas, is the average of the rate constants for the 200 Torr data and for the 300 Torr data. The uncertainty in K results from the 20% systematic uncertainty, the statistical uncertainty in the rate constants determined by the least-squares fit, and the 5% uncertainty in subtracting out the background decay rate.

Referring to equations 1 and 2, the quenching of a $He_2(a^3\Sigma_u^+)$ molecules by X results from either the bimolecular reaction

$$He_2(a^3\Sigma_u^+) + X \rightarrow \text{ Products (rate constant } K_2) \qquad (4)$$

or from the termolecular reaction

$$He_2(a^3\Sigma_u^+) + X + He \rightarrow \text{products (rate constant } K_3) \qquad (5)$$

In the collision between the $a^3\Sigma_u^+$ molecule and X, the long range radial potential is the sum of the Van der Waal attraction and the centrifugal potential. If the reactants do not have enough center of mass kinetic energy to surmount the centrifugal barrier, a glancing collision occurs. If the reactants can surmount the centrifugal barrier, the reactants come close together, spiralling about one another, with the activation energy determining the probability of a reaction. During the collision a third body, a $He_2(1^1S)$ atom for this experiment, may change the trajectory and the kinetic energy of the reactants enhancing the likelihood of spiralling collisions.

In describing the collisions of foreign gas molecules with $He(2^3S)$ atoms and with He_2^+ ions, Collins and Lee[6,11] calculate classical three-body capture

rates that agree fairly well with their measurements of termolecular rate constants for the respective collisions. Since the polarization potentials are not known for interactions between $He_2(a^3\Sigma_u^+)$ molecules and other molecules, similar calculations for collisions with $a^3\Sigma_u^+$ molecules have not been done.

From previous work on collisional quenching of $He(2^3S)$ atoms[4,5] and $He_2(a^3\Sigma_u^+)$ molecules[8] and consistent with our results, the changing of the He pressure in the discharge from 200 Torr to 300 Torr while holding the partial pressure of the foreign gas constant results in about a 5% increase in the effective rate constant. The pressure range used in this experiment is too small to permit an accurate determination of both the bimolecular and the termolecular rate constants from the measured effective rate constants. Data points from measurements of $a^3\Sigma_u^+$ decay rates at He pressures between 1,500 and 2,500 Torr are given for N_2 partial pressure of 14, 50, and 75 mTorr by Lee and Collins[8] and for Ar partial pressures of 15 and 50 mTorr by Lee et al.[10] We combine our data and their data in our analysis.

Figure 5, which is a plot of $a^3\Sigma_u^+$ decay rate as a function of the He pressure after the background decay rate has been subtracted out, shows the data points given by Lee and Collins for 14, 50, and 75 mTorr partial pressures of N_2. The low helium pressure data points are generated by multiplying the rate constants obtained from our measurements at 200 and 300 Torr by the partial pressure of N_2. The termolecular rate constant K_3 is determined by a least squares fit of the higher helium pressure data points to the expression

$$\frac{R}{[N_2]} = K + K_3 ([He] - [He]_o) \qquad (6)$$

where R is the $a^3\Sigma_u^+$ decay rate, $[N_2]$ is the N_2 concentration, K is the effective rate constant determined from our low pressure data, 1.6×10^{-10} cm^3 sec^{-1}, and $[He]_o = 8.25 \times 10^{18}$ cm^{-3} is the concentration of He atoms in a room temperature

gas at 250 Torr. The bimolecular rate constant K_2 is given by

$$K_2 = K - K_3 [He]_o. \quad (7)$$

The uncertainty assigned K_3 is one half the difference in the slope of the shallowest and steepest lines that bound the data. At the high He pressures used by Lee and Collins, the processes causing source and loss terms evolve rapidly so, that, during the decay of the $a^3\Sigma_u^+$ population in the afterglow, systematic effects are small compared to the statistical scatter of the data. The uncertainty assigned to K_2 is equal to the uncertainty in K. This gives $K_2 = (1.5 \pm 0.4) \times 10^{-10}$ cm^3 sec^{-1} and $K_3 = (2.3 \pm 0.9) \times 10^{-30}$ cm^6 sec^{-1} for N_2. The solid lines in Fig. 6 are generated from the bimolecular and termolecular rate constants given above for N_2. The dashed lines indicate the product of the partial pressure of N_2 times the effective rate constant given in Ref. 8 for He pressures in the range from 1,500 to 2,500 Torr.

We use the same procedure to obtain K_2 and K_3 from our Ar data and the Ar data of Lee et al.[10] This gives $K_2 = (5.9 \pm 2.4) \times 10^{-11}$ cm^3 sec^{-1} and $K_3 = (4.4 \pm 1.6) \times 10^{-30}$ cm^6 sec^{-1}. Lee et al use a previous low He pressure measurement by Pitchford and Deloche[9] of the rate constant for quenching of $a^3\Sigma_u^+$ molecules by Ar to determine $K_2 = (1.5 \pm 0.3) \times 10^{-10}$ cm^3 sec^{-1} and $K_3 = (2.4 \pm 0.9) \times 10^{-30}$ cm^6 sec^{-1}. A possible reason why our analysis and that of Lee et al[10] gives different values for K_2 and K_3 is given at the end of this section.

Because Lee and Collins do not show their data for CO_2, we estimate the bimolecular and termolecular rate constants using a different method. They give the effective bimolecular rate constant for the quenching of $a^3\Sigma_u^+$ molecules by CO_2 at helium pressures between 1,500 Torr and 2,500 Torr as $(9.5 \pm 2.8) \times 10^{-10}$ cm^3 sec^{-1}. Using our effective rate constant at 250 Torr for CO_2, $(6.4 \pm 1.8) \times 10^{-10}$ cm^3 sec^{-1}, we solve the following equations

$$6.4 \times 10^{-10}\ cm^3\ sec^{-1} = K_2 + K_3\ (250)(3.3 \times 10^{16}\ cm^{-3}) \quad (8)$$

and

$$9.5 \times 10^{-10}\ cm^3\ sec^{-1} = K_2 + K_3\ (2000)\ (3.3 \times 10^{16}\ cm^{-3}). \quad (9)$$

This gives $K_2 = (5.9 \pm 1.8) \times 10^{-10}\ cm^3\ sec^{-1}$ and $K_3 = (5.4 \pm 2.1) \times 10^{-30}\ cm^6\ sec^{-1}$ where the uncertainty in K_2 is set equal to the uncertainty in K and the relative uncertainty in K_3 is set equal to the relative uncertainty in K_3 for N_2, about 40%. These results for N_2, Ar, and CO_2 are summarized in Table I.

Direct comparison with other experiments is not possible except in the case of Ar. For N_2, O_2, and H_2, the rate constants for the quenching of $a^3\Sigma_u^+$ molecules seem reasonable, being 1.5 to 3 times larger than the corresponding rate constants for the destruction of 2^3S atoms. The bimolecular and termolecular rate constants calculated from the data of this experiment combined with the data of Lee and Collins for quenching of $a^3\Sigma_u^+$ molecules by N_2 are quite similar to the rate constants measured by Lee et al[10] for quenching of $a^3\Sigma_u^+$ molecules by Ar. This similarity in value is also seen in the rate constants for the quenching of $He(2^3S)$ atoms by Ar and by N_2. The bimolecular rate constant that we calculate for the quenching of $a^3\Sigma_u^+$ molecules by CO_2 is slightly smaller than the corresponding rate constant for quenching of 2^3S atoms. However, when one considers the uncertainties given for the CO_2 measurements, the small difference is not significant.

Lindinger et al[3] observe that the collisional quenching rate constants for $He(2^3S)$ atoms by various gases yield reasonably straight lines for Arrhenius plots. They calculate activation energies for the quenching of 2^3S atoms by H_2, N_2, Ar, O_2, and CO_2 of 72, 59, 59, 36, and 19 mV, respectively. If

the activation energies for the quenching of $a^3\Sigma_u^+$ molecules by these five gases all scale downward by the same factor from their respective values for the quenching of 2^3S atoms, the relative increase in the rate constant would be greatest for H_2 and progressively less for N_2, Ar, O_2, and CO_2 with the relative change in Ar and N_2 being the same. This behavior is consistent with our measurements if one uses the value of Lee et al[10] for Ar instead of the one determined in this work. Testing this speculation that all the activation energies scale downward by approximately the same factor would require measuring the rate constants over a range of temperatures, an experiment not possible with our apparatus.

As a final point, there is a large disagreement between this work and that of Lee et al in the rate constant measured for Ar. The recombination coefficient at room temperature for Ar^+ ions is quite small,[14] 6×10^{-10} cm^3 sec^{-1}. Since the second ionization potential[15] of Ar is larger than the energy stored in either the $He(2^3S)$ or the $He_2(a^3\Sigma_u^+)$ metastables, Ar^+ ions do not readily react with He metastables. Measurements in this work are performed later in the afterglow than those of Lee et al. Conversion of Ar atoms to Ar^+ ions by collisions with He metastables could reduce the concentration of Ar atoms in the later afterglow enough to reduce the measured rate constants for the quenching of $a^3\Sigma_u^+$ molecules. This possible problem does not arise for the other molecules used in our experiments. For example, the recombination coefficients for N_2 and O_2 are 2.0×10^{-7} and 2.2×10^{-7} cm^3 sec^{-1}, respectively.[16]

References

1. W. S. Steets and N. F. Lane, Phys. Rev. A11, (1975).
2. J. S. Cohen, Phys. Rev. A 13, 86 (1976).
3. W. Lindinger, A. L. Schmeltekopf, and F. C. Fehsenfeld, J. Chem. Phys. 61, 2890 (1974).
4. F. W. Lee and C. B. Collins, J. Chem. Phys. 65, 5189 (1976).
5. C. B. Collins and F. W. Lee, J. Chem. Phys. 70, 1275 (1976).
6. J. E. Lawler, J. W. Parker, L. W. Anderson and W. A. Fitzsimmons, IEEE J. of Quantum Electronics QE-15, 609 (1979).
7. A. C. G. Mitchell and M. W. Zemansky, Resonance Radiation and Excited Atoms, (Cambridge Univ. Press, N.Y., 1961), p. 192.
8. F. W. Lee and C. B. Collins, J. Chem. Phys. 67, 2798 (1977).
9. L. C. Pitchford and R. Deloche, J. Chem. Phys. 68, 1185 (1978).
10. F. W. Lee, C. B. Collins, L. C. Pitchford, and R. Deloche, J. Chem. Phys. 68, 3025 (1978).
11. J. W. Parker, Ph.D. thesis, University of Wisconsin, unpublished (1980).
12. A. B. Callear and R. E. M. Hedges, Trans. Faraday Soc. 66, 2921 (1970).
13. C. B. Collins and F. W. Lee, J. Chem. Phys. 68, 1391 (1978).
14. M. A. Biondi, Phys. Rev. 129, 1171 (1963).
15. G. Herzberg, Atomic Spectra and Atomic Structure, New York, New York: Dover Publications, Inc., 1937, p. 200.
16. J. Dutton, J. Phys. Chem. Ref. Data 4, 577 (1974).

Table I.

Rate constants[a] for quenching of $He_2(a^3\Sigma_u^+)$ metastable molecules and $He(2^3S)$ metastable atoms at room temperature.

$He_2(a^3\Sigma_u^+)$

X	K[b]	K[c]	K_2[d]	K_3[d]	K_2[e]	K_3[e]
Ar	9.1±2.8	31±9	5.9±2.8	4.4±1.6	15±3	2.4±0.8
N_2	16 ±4.7	30±9	15 ±4.7	2.3±0.9		
O_2	27 ±9.3					
H_2	11 ±3.5					
CO_2	64 ±21	95±28	59 ±21	5.4±2.1		

$He(2^3S)$

X	K_2[f]	K_2[g]	K_3[g]
Ar	7.1±2.1	7.5±2.0	2.2±0.7
N_2	7.1±2.1	6.9±2.1	2.9±0.7
O_2	24.5±7.4	19 ±6	3.1±1.2
H_2	2.9±0.9	3.8±1.1	1.2±0.3
CO_2	65 ±20	70 ±21	8.3±1.0

[a] K and K_2 are in units of 10^{-11} cm^3 sec^{-1} and K_3 is in units of 10^{-30} cm^6 sec^{-1}.

[b] This work.

[c] From Ref. 8.

[d] This work combined with Ref. 8.

[e] From Ref. 10.

[f] From Refs. 3-6.

[g] From Refs. 4 and 5.

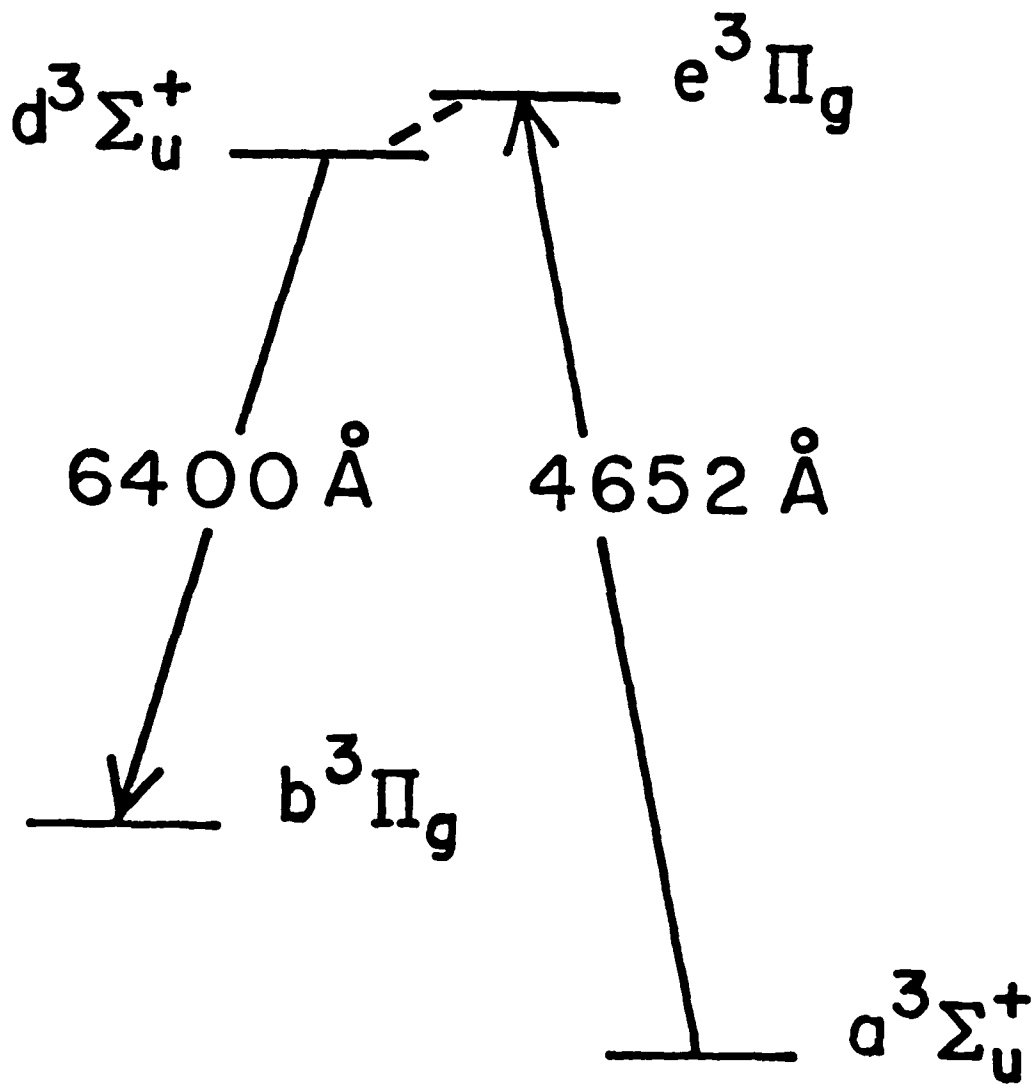

FIG. 1. Simplified energy level diagram for He_2 molecules showing the energy separation of the v = 0 vibrational levels of the electronic configuration relevent to this paper.

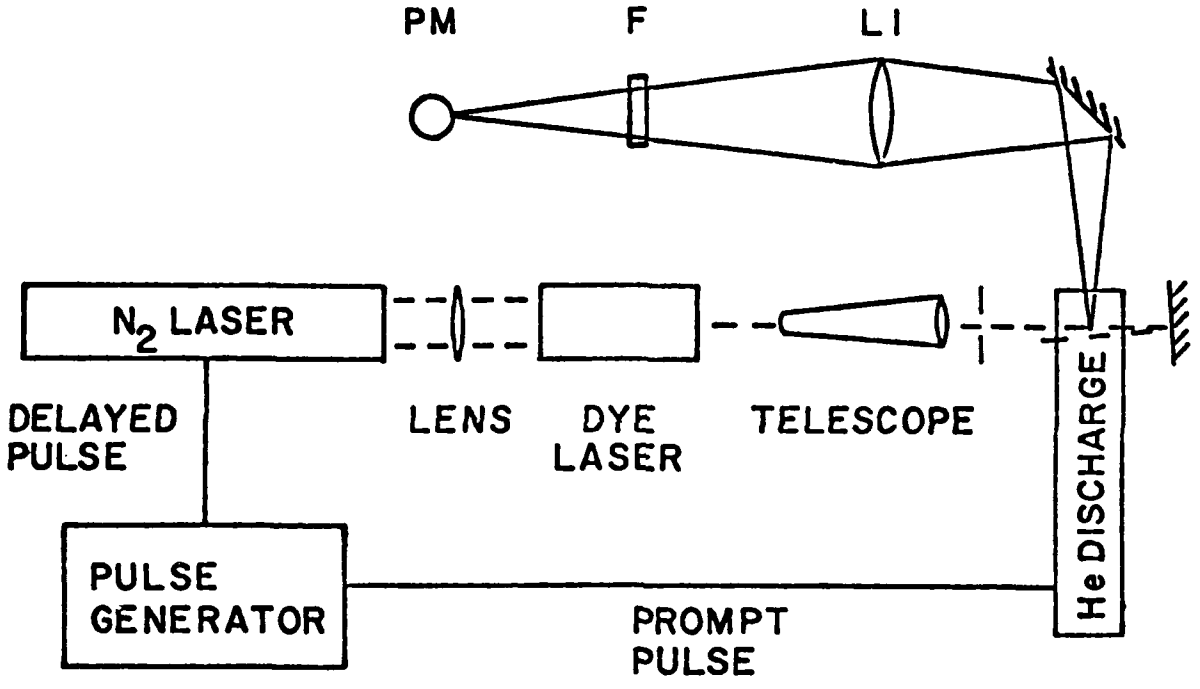

FIG. 2. Schematic diagram of the experimental apparatus. A N_2 laser pumps a dye laser. The dye-laser radiation is collimated by a telescope and then passed through the He discharge. Dye-laser induced fluorescence is imaged onto the cathode of a photomultiplier tube PM by lens L1.

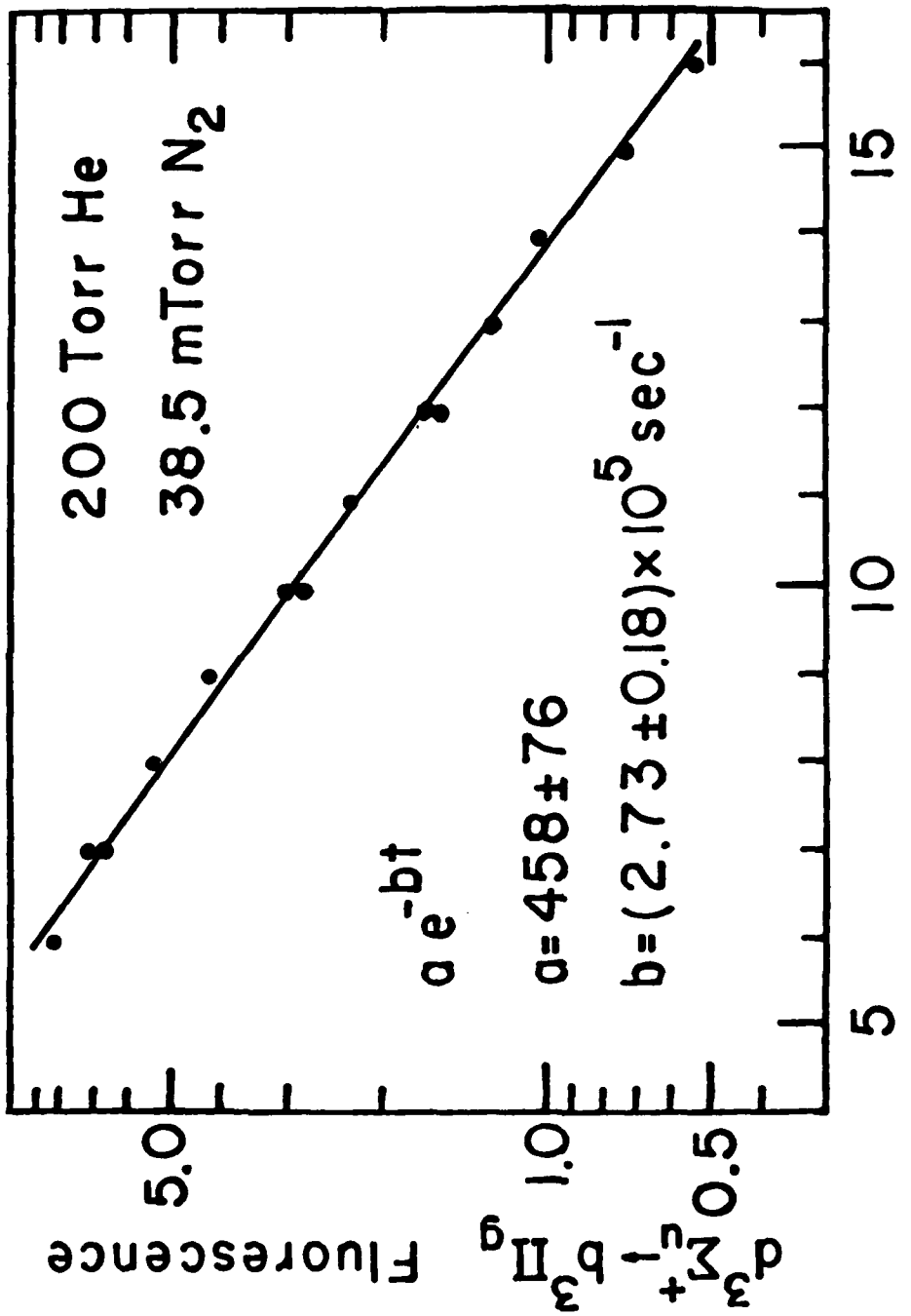

FIG. 3. Data plot of the laser-induced fluorescence signal as a function of delay in the afterglow. The data for this plot are taken for a 200 Torr He discharge with a 38.5 m Torr N_2 partial pressure.

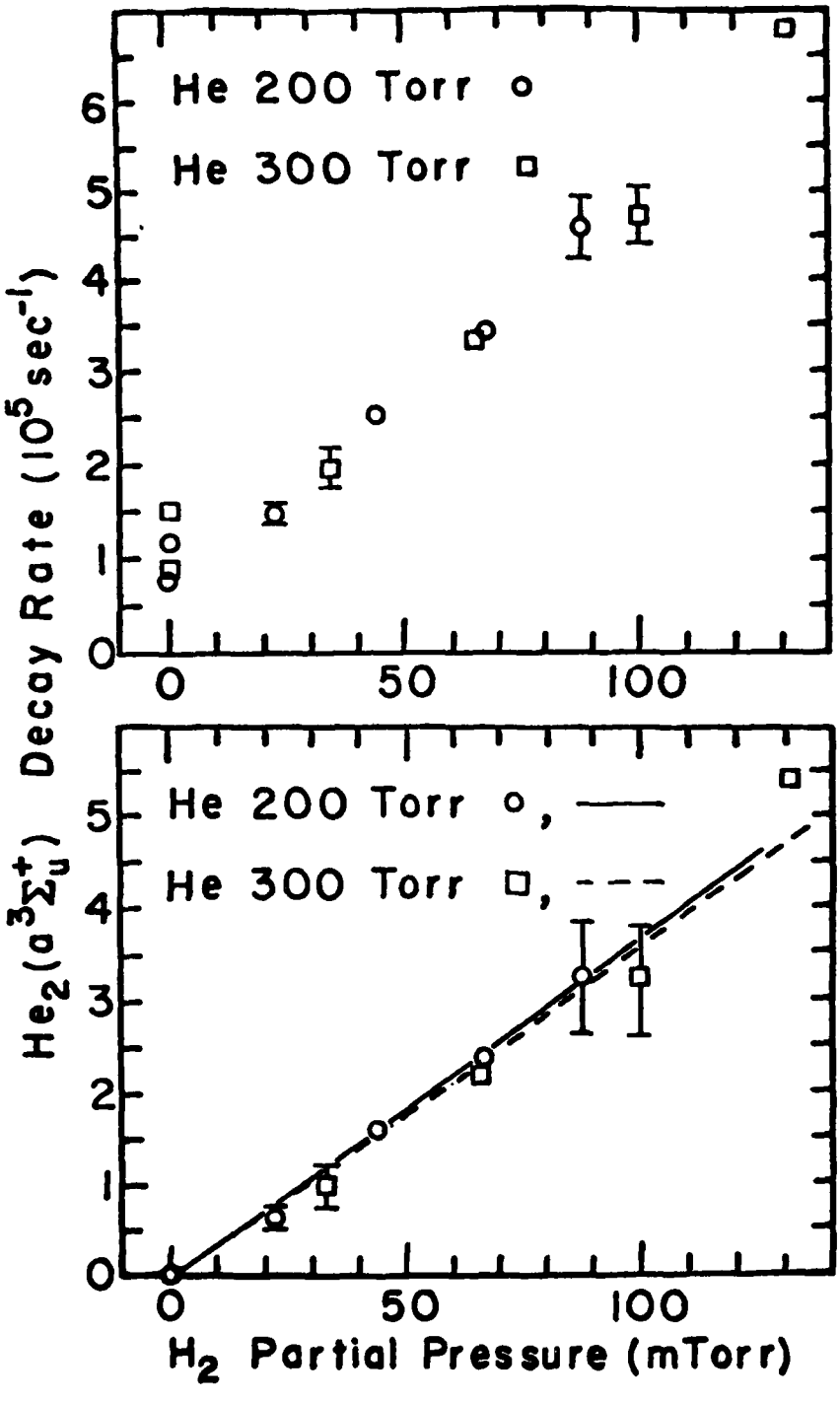

FIG. 4. Upper plot: measured $a^3\Sigma_u^+$ decay rate versus partial pressures of H_2. Lower plot: Stern-Volmer plot of $a^3\Sigma_u^+$ decay rate after background is subtracted out.

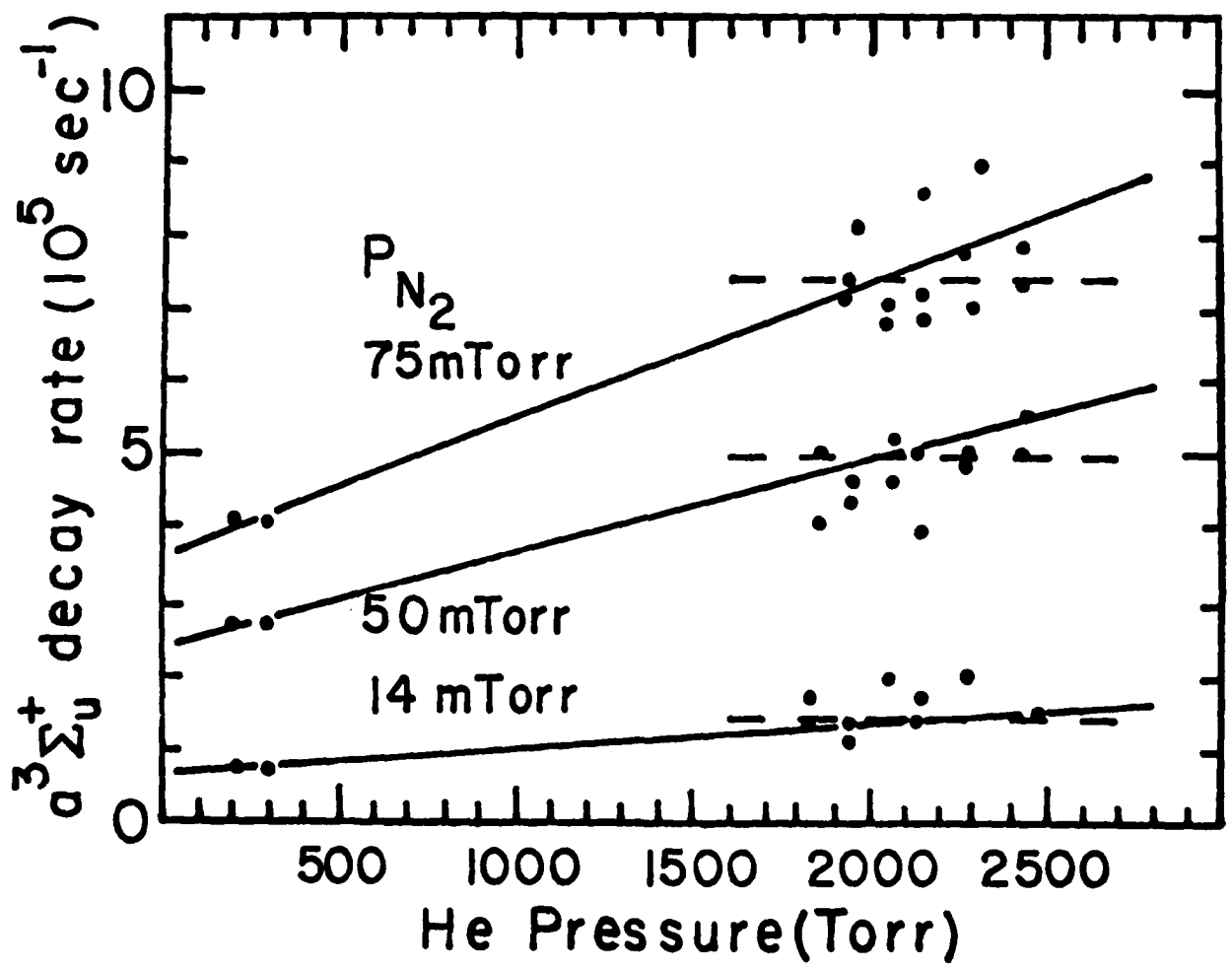

FIG. 5. Plot of $a^3\Sigma_u^+$ decay rate versus He pressure for 14, 50, and 75 m Torr partial pressure of N_2. The high He pressure points are the data points given in Fig. 2 of Ref. 8 with the background decay rate subtracted out. The low He pressure points are the product of the rate constants obtained by our measurements at 200 and 300 Torr times the partial pressure of N_2. The solid lines are generated from the bimolecular and termolecular rate constants obtained from Eqs. (6) and (7). The dashed lines indicate the product of the partial pressure of N_2 times the effective bimolecular rate constant given in Ref. 8 for He pressure in the range from 1500 to 2500 Torr.

Chapter IV.

The electron excitation of N_2 molecules

Measurements of the absorption and emission intensities of various electronic transitions and their time-dependence in a pulsed electron-excited N_2 experiment furnish an effective means of probing collisional energy transfer processes. In order to extract the rate constants for the transfer processes it is important to know the direct electron excitation cross sections of the low excited electronic states, especially the triplet series. Measurements of the excitation cross sections for the $B^3\Pi_g$ and $C^3\Pi_u$ levels by the optical method have been reported from several laboratories, but much less is known about the $A^3\Sigma_u^+$ level. This level is metastable and play an important role in many atmospheric and laboratory processes. The first step of our effort in this phase of the work is to measure the electron excitation cross section of the $A^3\Sigma_u^+$ level of N_2.

The electron excitation of many N_2 levels can be studied by measuring the emission intensity from these excited levels. The $A^3\Sigma$ level of N_2 is, however, metastable so that emission studies are very difficult. Thus a different method is desirable to study the electron excitation of the $A^3\Sigma$ level of N_2. We have used the laser induced fluorescence method for attempting to study the excitation of the $A^3\Sigma$ level.

Our apparatus is shown schematically in Fig. 1. The laser induced fluorescence method works as follows. A vacuum chamber contains a low density of N_2 gas (1 - 30 mTorr). An electron beam passes through the low density N_2 gas. The electron beam is formed from an indirectly heated cathode and is extracted and focussed into a parallel beam with a diameter of about 2 mm using a number of electrodes. The energy of the electron beam is variable from a few eV to about 300 eV. The voltage that determines the energy of the electron beam is used to drive the x input of an x-y recorder. The electron beam collisionally excites some of the N_2 molecules to various excited energy

levels including the $A^3\Sigma$ level. Some of the $A^3\Sigma$ molecules formed result from the direct electron excitation process and others result from the excitation of high levels that produce $A^3\Sigma$ level molecules by cascading. A dye laser beam is normally incident on the electron beam. The dye laser beam is tuned so that the wavelength corresponds to a particular $A^3\Sigma \rightarrow B^3\Pi$ vibration rotation transition. The $B^3\Pi$ level molecules thus formed radiate. The $B^3\Pi$ laser induced fluorescence is observed along an axis that is perpendicular to both the electron beam and the laser beam. The electron excitation cross section of the $A^3\Sigma$ level can be obtained from measurements of the laser-induced fluorescence from the $B^3\Pi$ level.

We initially used a Spectra Physics broad band cw dye laser pumped by a Spectra Physics 9W Argon ion laser for our experiments. The laser induced fluorescence was analyzed using a Jobin-Yvon 1-m spectrometer and detected using a photomultiplier. The laser beam is chopped at about 720 Hz. A signal from the chopper serves as the reference for a lock-in amplifier. The output of the photomultiplier serves as the input signal for the lock-in amplifier. It can be shown that the lock-in amplifier signal is directly proportional to the apparent cross section for the electron excitation of the particular $A^3\Sigma$ vibration rotation level under study. The output of the lock-in amplifier is used to drive the y-input of the x-y recorder. Thus the apparent cross section for the electron excitation of the particular $A^3\Sigma$ vibration-rotation level under study is plotted as a function of the energy on the x-y plotter. After passing through the vacuum chamber the dye laser beam is incident on a N_2 discharge. The N_2 discharge was obtained using an old He-Ne laser tube attached to a vacuum system. The He-Ne laser tube is evacuated and then filled to a pressure of about 100 mTorr with N_2. A dc discharge is ignited using the electrodes of the He-Ne tube. When the

dye laser wavelength corresponds to the wavelength for the absorption of one of the $A^3\Sigma \rightarrow B^3\Pi$ transition then the i-v characteristic of the N_2 discharge is altered by the optogalvanic effect. An oscilloscope monitors the voltage across the N_2 discharge. Using the optogalvanic effect in this manner it is possible to set the laser wavelength so that it corresponds to the wavelength of the particular $A^3\Sigma \rightarrow B^3\Pi$ transition under study. We have found that it is possible to observe hundreds of $A^3\Sigma \rightarrow B^3\Pi$ transitions using the optogalvanic effect.

It was stated that it can be shown that the output of the lock-in amplifier is directly proportional to the apparent cross section for the production of the particular $A^3\Sigma$ vibration-rotation level under study. In order to show this important result it is necessary to carry out a rate equation analysis. We denote the $A^3\Sigma$ vibration level under study by "a". The $A^3\Sigma \rightarrow B^3\Pi$ absorption induced by the dye laser leads to a $B^3\Pi$ vibration-rotation level we denote by "b". The rate equations for levels "a" and "b" are given by

$$\frac{dn_a}{dt} = \left(\frac{nJ}{e}\right)Q_a - n_a A_a + n_b A_{ba} + \sum_{\substack{j>a \\ j\neq b}} n_j A_{ja} - B_{ab}\rho n_a + B_{ba}\rho n_b, \qquad (1)$$

and

$$\frac{dn_b}{dt} = \left(\frac{nJ}{e}\right)Q_b - n_b A_b + \sum_{j>b} n_j A_{jb} + B_{ab}\rho n_a - B_{ba}\rho n_b , \qquad (2)$$

where n is the ground level N_2 density, J is the electron current density, Q_i is the direct electron excitation cross section for level i, A_a is the reciprocal of the beam crossing time for the metastable $A^3\Sigma$ level, A_b is the reciprocal of the lifetime of the $B^3\Pi$ level, A_{ij} is the radiative decay rate of level "i" into level "j", B_{ab} is the Einstein coefficient for induced

absorption, B_{ba} is the Einstein coefficient for induced emission, and ρ is the energy density in the laser beam. It is well known that the Einstein B coefficients are related by $B_{ab} = B_{ba}(g_b/g_a)$ where g_a and g_b are the statistical weights of the levels "a" and "b" respectively. Note that $A_a << A_b$ since level "a" is metastable whereas level "b" can radiate. The steady state solution to equations (1) and (2) is

$$n_{b\text{-}on} = \left(\frac{nJ}{e}\right) \frac{[Q_b^A + \gamma(Q_a^A - Q_{ba})]}{[(A_b + B_{ba}\rho) - \gamma(A_{ba} + B_{ba}\rho)]},$$

where Q_a^A and Q_b^A are called the apparent cross sections and are given by $Q_a^A = Q_a + \sum_{j>a} Q_{ja}$ and $Q_b^A = Q_b + \sum_{j>b} Q_{jb}$. The quantities Q_{ja} and Q_{jb} are called optical cross section and are given by $Q_{ja} = \left(\frac{e}{nJ}\right)n_j A_{ja}$ and $Q_{jb} = \left(\frac{e}{nJ}\right)n_j A_{jb}$. The apparent cross section is the sum of the direct cross section plus the sum of the optical cross sections so that Q_a^A includes direct production plus cascading. The quantity γ is given by $\gamma = B_{ab}\rho/(A_a + B_{ba}\rho)$. The subscript "on" indicates that the laser is on. When the laser is off then $\rho = 0$. The value of n_b when the laser is off is given by $n_{b\text{-}off} = \left(\frac{nJ}{e}\right)\left(\frac{Q_b^A}{A_b}\right)$. Our initial experiments employ a broadband cw dye laser with a bandwidth of $1.5 - 4 \times 10^{10}$ Hz. The longitudinal mode separation is 4.20×10^8 Hz. Thus there are 30-100 modes in the laser bandwidth. Not all the modes lase simultaneously and in fact at a given time only one or a few modes may be lasing. The modes that are lasing change in time so that a given mode lases only part of the time. The Doppler width of a N_2 $A^3\Sigma \rightarrow B^3\Pi$ transition is about 1.0×10^9 Hz which is much less than the bandwidth of the laser. Even when the laser is tuned so that a Doppler broadened $A^3\Sigma \rightarrow B^3\Pi$ transition is covered by the laser bandwidth the laser modes that interact with the transition may not be lasing. When a laser mode that interacts with the

transition is lasing the intensity of the mode is high enough to saturate the transition i.e. $B_{ab}\rho >> A_a$. Thus when a laser mode that interacts with the transition is lasing then

$$N_{b\text{-}on} = \left(\frac{nJ}{e}\right) \frac{Q_b^A + Q_a^A - Q_{ba}}{(A_b - A_{ba})}$$

where we have used the result $A_b >> A_a$.

The fluorescence signal when the laser is off or when the laser is lasing but none of the lasing modes interacts with the transition is proportional to $n_{b\text{-}off}$. The fluorescence signal when a lasing mode interacts with the transition is proportional to $n_{b\text{-}on}$. Thus the fluorescence signal when the laser is on is

$$S_{on} \propto \beta n_{b\text{-}on} + (1 - \beta) n_{b\text{-}off}$$

where β is a constant determined by the time average of the laser intensity, and the fluorescence signal when the laser is off is

$$S_{off} \propto n_{b\text{-}off} .$$

The difference between S_{on} and S_{off} is

$$S_{on} - S_{off} \propto \beta(n_{b\text{-}on} - n_{b\text{-}off}) = \beta \frac{nJ}{e}\left[\frac{Q_a^A}{(A_{ba} - A_{ba})}\right].$$

Thus we have shown that as stated $S_{on} - S_{off}$ is directly proportional to Q_a^A. A measurement of $S_{on} - S_{off}$ will yield the energy dependence of Q_a^A. An absolute calibration of Q_a^A must be made. For our previous measurements on Ne we have calibrated the pure triplet cross sections[1] by use of the fact that the direct cross section for a triplet excitation falls to near zero above about 65 eV and hence Q_a^A is equal to the cascade contribution at higher energies. Thus by measuring the cascades absolutely the absolute

value of Q_a^A can be obtained above 65 eV. For our measurements on N_2 this will probably not be possible so we hope to use a laser intense enough to excite all the $A^3\Sigma$ molecules and to calibrate the absolute cross section in terms of the absolute value of the laser induced fluorescence.

We have attempted to measure the value of apparent cross section of many different vibration rotation levels of the $A^3\Sigma$ level. We have been unable to detect any laser induced fluorescence no matter what the initial vibration rotation level of the $A^3\Sigma$ levels using a multimode laser. Because the modes of a multimode laser do not necessarily lase all the time the laser does not fully interact with the level under study. In order to rectify this problem we have set up a single mode ring dye laser and have attempted to measure the laser induced fluorescence using it. Again the results were negative. Since we have previously observed very strong signals from the laser induced fluorescence when studying the Ne metastable levels we must ask "Why is no signal detected?" We believe that the reason we do not detect a signal for N_2 is that there are so many vibration-rotation levels in the $A^3\Sigma$ level that the population due to any individual level is too small to produce an observable laser-induced fluorescence signal.

One possible way to resolve this difficulty is to use a light source with a bandwidth wide enough to pump all the rotational levels associated with a given vibrational level of the $A^3\Sigma_u^+$ electronic level. A pulsed dye laser does not have well defined modes so all the rotation levels may interact with the laser. A N_2 laser pumped dye laser can easily have enough power to saturate all the N_2 molecules in all the rotational levels associated with a given vibration level. Although we have not yet been successful in measuring the electron excitation cross sections for the metastable $A^3\Sigma$

level of the N_2 molecule, we suggest that the scheme outlined above is a promising method for molecular metastable levels. Once the fundamental cross sections are determined, it is possible to study the reactions that occur in a pulsed N_2 system. The processes include the production of the $A^3\Sigma$, $B^3\Pi$, and $C^3\Pi$ levels and the various quenching and excitation transfer reactions that follow their production.

References

1. M. H. Phillips, L. W. Anderson, and C. C. Lin, Phys. Rev. A 23, 2751 (1981); M. H. Phillips, L. W. Anderson, C. C. Lin, and R. E. Miers, Phys. Lett. 82A, 404 (1981).

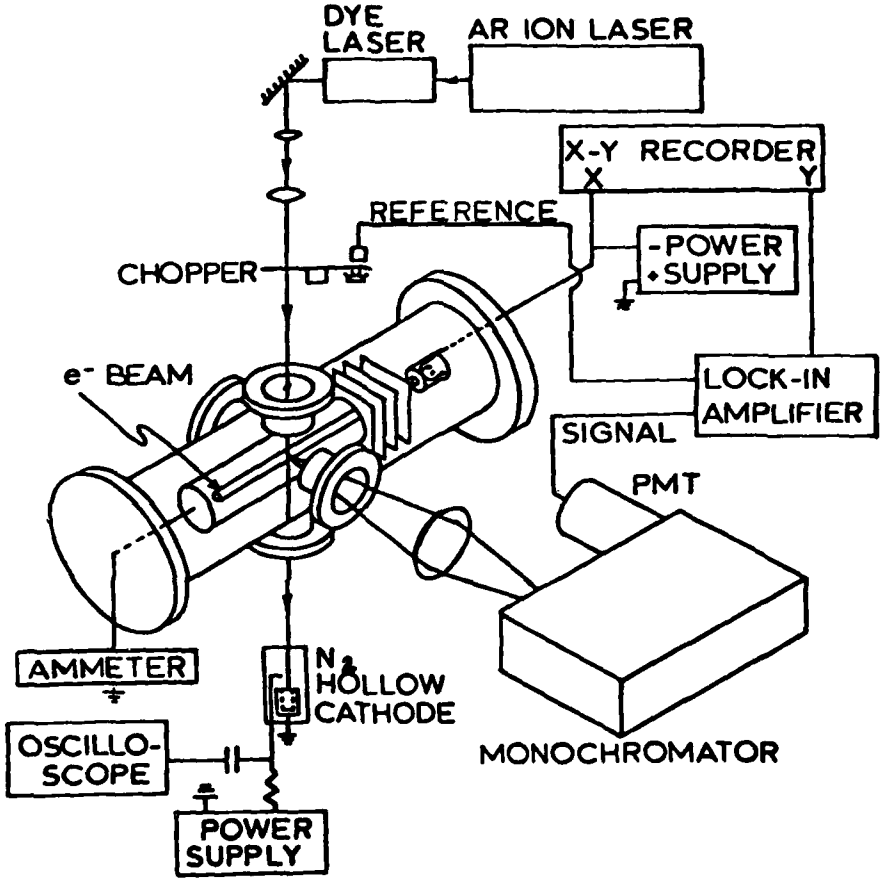

FIG. 1. A schematic diagram of our apparatus.

Publications

The works reported in the following papers were partially supported by this contract:

"$He_2(d^3\Sigma_u^+)$ Decay Rate in a High-Pressure Helium Afterglow", Journal of Chemical Physics 73, 6179 (1980).

"Collisional Quenching of He_2 Molecules in the $a^3\Sigma_u^+$ Level by Impurity Gases", Journal of Chemical Physics 75, 1804 (1981).